HHS Public Access

Author manuscript

Mol Cell Endocrinol. Author manuscript; available in PMC 2017 December 05.

Published in final edited form as:

Mol Cell Endocrinol. 2016 December 5; 437: 224–236. doi:10.1016/j.mce.2016.08.031.

Evaluation of *in vivo* bioactivities of recombinant hypo- ($FSH^{21/18}$) and fully- (FSH^{24}) glycosylated human FSH glycoforms in *Fshb* null mice

Huizhen Wang[a], **Jacob May**[a], **Viktor Butnev**[f], **Bin Shuai**[f], **Jeffrey V. May**[f], **George R. Bousfield**[f], and **T. Rajendra Kumar**[a,b,c,d,e,*]

[a]Department of Molecular and Integrative Physiology, University of Kansas Medical Center, Kansas City, KS 66160, USA

[b]Center for Reproductive Sciences, Institute for Reproductive Health and Regenerative Medicine, University of Kansas Medical Center, Kansas City, KS 66160, USA

[c]Department of Pathology and Laboratory Medicine, University of Kansas Medical Center, Kansas City, KS 66160, USA

[d]Department of Neurosurgery, University of Kansas Medical Center, Kansas City, KS 66160, USA

[e]Division of Reproductive Sciences, Department of Obstetrics & Gynecology, University of Colorado Denver-Anschutz Medical Campus, Aurora, CO 80045, USA

[f]Department of Biological Sciences, Wichita State University, Wichita, KS 67260, USA

Abstract

The hormone - specific FSHβ subunit of the human FSH heterodimer consists of N-linked glycans at Asn^{7} and Asn^{24} residues that are co-translationally attached early during subunit biosynthesis. Differences in the number of N-glycans (none, one or two) on the human FSHβ subunit contribute to macroheterogeneity in the FSH heterodimer. The resulting FSH glycoforms are termed hypo-glycosylated ($FSH^{21/18}$, missing either an Asn^{24} or Asn^{7} N-glycan chain on the β - subunit, respectively) or fully glycosylated (FSH^{24}, possessing of both Asn^{7} and Asn^{24} N-linked glycans on the β - subunit) FSH. The recombinant versions of human FSH glycoforms ($FSH^{21/18}$ and FSH^{24}) have been purified and biochemically characterized. *In vitro* functional studies have indicated that $FSH^{21/18}$ exhibits faster FSH- receptor binding kinetics and is much more active than FSH^{24} in every assay tested to date. However, the *in vivo* bioactivity of the hypoglycosylated FSH glycoform has never been tested. Here, we evaluated the *in vivo* bioactivities of FSH glycoforms in *Fshb* null mice using a pharmacological rescue approach. In *Fshb* null female mice, both hypo- and fully-glycosylated FSH elicited an ovarian weight gain response by 48h and induced ovarian genes in a dose- and time-dependent manner. Quantification by real time qPCR

*Corresponding author. Department of Obstetrics & Gynecology, University of Colorado Denver-Anschutz Medical Campus, Aurora, CO 80045, USA. raj.kumar@ucdenver.edu (T.R. Kumar). .

Disclosure statement: The authors have nothing to disclose

assays indicated that hypo-glycosylated $FSH^{21/18}$ was bioactive *in vivo* and induced FSH-responsive ovarian genes similar to fully-glycosylated FSH^{24}. Western blot analyses followed by densitometry of key signaling components downstream of the FSH-receptor confirmed that the hypo-glycosylated $FSH^{21/18}$ elicited a response similar to that by fully-glycosylated FSH^{24} in ovaries of *Fshb* null mice. When injected into *Fshb* null males, hypo-glycosylated $FSH^{21/18}$ was more active than the fully-glycosylated FSH^{24} in inducing FSH-responsive genes and Sertoli cell proliferation. Thus, our data establish that recombinant hypo-glycosylated human $FSH^{21/18}$ glycoform elicits bioactivity *in vivo* similar to the fully-glycosylated FSH. Our studies may have clinical implications particularly in formulating FSH-based ovarian follicle induction protocols using a combination of different human FSH glycoforms.

Keywords

FSH-responsive genes; N-glycosylation; Ovary; Testis; Pharmacological rescue

1. Introduction

Follicle-stimulating hormone (FSH) is synthesized in and secreted from pituitary gonadotropes [1, 2]. FSH and other pituitary (LH and TSH) and placental (hCG) glycoprotein hormones contain two non-covalently associated heterodimeric α– and β–subunits [1, 2]. Both the common α–subunit and hormone-specific FSHβ, possesses up to 2 N-linked glycan chains [1-3]. The co-translational addition of $GlcNAC_2$ Man_9Glc_2 precursors to conserved Asn residues and subsequent post-translational conversion of each precursor to complex-type glycan structures constitute a multi-enzyme driven process termed N-glycosylation that occurs in the ER-Golgi compartments [1-3]. Recent structural studies revealed differences in N-glycan chain number, sugar composition and branching pattern of the mature human FSH purified from pooled pituitary glands, pooled postmenopausal urine, or produced *in vitro* using a CHO cell expression system [4-11].

Previous studies have identified differences in the abundance of different FSH glycoforms as a function of age [12-16]. It was predicted that such age-related FSH glycoforms act differently in different target cells [4, 14, 17]. Direct purification of FSH glycoforms from human pituitaries and/or urine collected at different ages and their characterization indeed identified hypo-glycosylated FSH is a mixture of FSH^{18} and FSH^{21} glycoforms present as the dominant form in young age and fully-glycosylated FSH, designated as FSH^{24} is the dominant form in old age [4, 6, 14, 17-20]. Recombinant expression in a heterologous GH_3 cell culture system followed by purification and biochemical characterization revealed that these FSH glycoforms differ in the number or location of N-linked glycan chains on FSHβ subunit [4-7, 14]. While both N-linked glycans are present at Asn^7 and Asn^{24} in the FSHβ subunit of fully-glycosylated FSH^{24}, a single N-linked glycan is present only at Asn^7 in the FSHβ subunit of FSH^{21} or at Asn^{24} in the FSHβ subunit of FSH^{18}. The latter two glycoforms are collectively known as hypo-glycosylated FSH and referred to as $FSH^{21/18}$ [4-7, 14, 19].

Both the pituitary-derived preparations and GH_3 cell-derived recombinant FSH glycoforms have been biochemically characterized *in vitro* and compared to fully-glycosylated FSH^{24} with regard to receptor binding and dissociation kinetics, glycan composition by mass spectrometry and *in vitro* bioactivity using radio-receptor assays [4-7, 14, 18, 19]. More recently, these FSH glycoforms have also been tested in an FSH-responsive KGN granulosa cell line [17]. However, the *in vivo* bioactivities of GH_3-derived recombinant human FSH glycoforms have not yet been directly tested. Moreover, whether hypoglycosylated FSH ($FSH^{21/18}$) elicits bioactivity *in vivo* is not yet known. Here, we have used a pharmacological rescue approach and injected the GH_3 cell-derived recombinant human $FSH^{21/18}$ and FSH^{24} glycoforms into our well characterized *Fshb* null mice [21-24] and directly assayed ovarian and testis gene expression changes as a measure of glycoform *in vivo* bioactivity. We demonstrate that recombinant hypo-glycosylated $FSH^{21/18}$ glycoform elicits FSH bioactivity *in vivo* in the absence of endogenous FSH.

2. Materials and Methods

2.1. Production of GH_3-derived recombinant human FSH glycoforms

Recombinant human FSH glycoforms were purified from rat pituitary GH_3 clones that co-express fully-glycosylated $hFSH^{24}$ and both hypo-glycosylated glycoforms $hFSH^{18}$ and $hFSH^{21}$ as a mixture (Fig. 1A). The purification and characterization of the hormones from GH_3-conditioned media were described in detail elsewhere [6, 17, 18]. Western blot analysis of FSH preparations was performed with the FSHβ subunit-specific primary antibody RFSH20 (1:5000) that detected two bands corresponding to 18 KDa and 21 KDa in the $FSH^{21/18}$ preparation (Fig.1B, Lane 1), and a single band at 24KDa in the case of FSH^{24} and hFSH AFP 7298 reference preparation (Fig. 1B, Lanes 2 and 3) as previously reported [6, 17, 18]. An independent blot similarly loaded as above with FSH preparations, was probed with an α-subunit antiserum, which detected a band in all the lanes (Fig. 1C). One μg aliquots of these purified and *in vitro* validated recombinant hormones were frozen and stored at −80C, thawed rapidly when required and immediately injected into mice. For the sake of simplicity, $FSH^{21/18}$ was referred to as FSH^{21}, the predominant glycoform in the $FSH^{21/18}$ mixture in all Figures.

2.2. Fshb null mice

Fshb null mice were generated and genotyped by genomic PCR assays performed on tail DNA samples as described before [23, 24]. For the *in vivo* bioactivity testing experiments, immature *Fshb* null female mice at 21d-22d of age or *Fshb* null male pups at postnatal day 3 or 5 were used. All mice were maintained under 12-h dark, 12-h light cycles with food and water supplied *ad libitum*. All studies with mice were performed in accordance with the Guide for the Care and Use of Laboratory Animals per the NIH instructions and approved institutional protocols.

2.3. Dose response study in the female

For the dose response study, *Fshb* null females were injected (i.p.) with different doses (0.5 μg, 1 μg or 2 μg) of purified recombinant hormones prepared in 100 μL of PBS or with 100 μL of PBS alone. These doses correspond to ~ 5, 10 and 20 IU respectively of the standard

reference human FSH preparation. Ovaries in each case were collected at different time points for either RNA, Western blot or immunofluorescence analysis as described below.

2.4. Time course study in the female

Three sets of experiments were designed. In the first set, mice were injected (i.p.) with different doses of purified recombinant hormones as described above, and ovaries were collected after 2h, 4h, 8h, 16h and 24h. In the second set, ovaries were collected after 0.5h, 1h and 2h. In the final set, ovaries were collected after 5 min, 10 min., and 20 min. For all experimental sets, ovaries, upon removal were immediately flash frozen on dry ice until further use and processed for either RNA or protein analysis.

2.5. In vivo bioassays in the male

For checking *in vivo* bioactivities of FSH glycoforms, the protocols indicated in Supplementary Fig. S1 were used. In one set of experiments (Supplementary Fig. S1 A, B), beginning postnatal day 5, pups were injected (i.p.) daily with 25 μL of either PBS or 1 μg of recombinant hormone ($FSH^{21/18}$ or FSH^{24}) for 5 days until postnatal day 9. On postnatal day 10, testes were collected and the wet weights recorded. One testis was fixed in formalin reagent for histological and immunochemical analysis and the other was snap frozen and processed for RNA isolation as described [24, 25]. In a second set of experiments (Supplementary Fig. S1 C), beginning postnatal day 3, mice were injected with PBS or glycoforms for 3 days - once daily on days 3, 4 and 5. On the morning of day 5, mice were injected with BrdU and after 2 h, blood and testes were collected and processed as described above.

2.6. RNA isolation, cDNA synthesis and Taqman Real-time qPCR assays

Total RNA was isolated from mouse ovaries or testis by RNEasy micro columns (Qiagen) and RNA quantified using a NanoDrop spectrophotometer (ThermoScientific) set at 260 nm. Approximately 500 ng-1 μg total RNA was reverse transcribed by the oligo dT method using the SuperScript III kit (ThermoScientific) as described [24-26]. Taqman real time qPCR assays were performed on the cDNA samples in triplicate using custom-made or pre-inventoried primer/combo mixes (ThermoScientific or IDT). Expression of *Ppil1* was used as an internal control and the relative amounts of mRNA expression were calculated as described [24-26].

2.7. Histological analysis

Testes and ovaries were processed, later paraffin-embedded and 6 μm sections were cut and stained with either PAS reagent/ hematoxylin or hematoxylin-eosin for histological analysis as described before [24-26]. Quantification of testis tubule size was done on PAS reagent / hemtoxylin – stained testis section images that were digitally captured as described [21]. Per group, three mice were used and ~ 100 tubules were counted in each case.

2.8 Immunofluorescence

Formalin-fixed and paraffin-embedded tissue sections of approximately 6μm thickness were cut and processed for immunofluorescence as described before [24-26]. The following

primary antibodies were used: rabbit polyclonal antibody against Sox9 (gift from Dr. K. Morohashi, 1:1,000), rat monoclonal antibody to GCNA (gift from Dr. George Enders, used undiluted) mouse anti BrdU monoclonal antibody (Roche, 1:100), rabbit anti phospho-CREB (Cell Signaling Systems) or rabbit anti phospho-PKA substrate (Cell Signaling Systems, 1:500) both at a dilution of 1:500. The sections were later incubated with the appropriate secondary antibodies conjugated with Alexa fluors (Invitrogen) and/or a nuclear dye and visualized using an epifluorescence microscope as described [24-26]. $GCNA^+$ germ cells were counted in ~ 100 tubules per group and three mice were used per group.

2.9. Western blot analysis

Gonadal proteins were extracted in immuno-precipitation buffer (Santa Cruz Biotechnology) and collected by centrifugation at 10,000 X g at 4C. Protein content was estimated by Bio-Rad protein assay using bovine serum albumin as standard. Aliquots of 10-15 μg of protein were denatured in SDS-PAGE sample buffer (final concentration = 32 mM Tris-HCl, pH 6.8, 12.5% glycerol (v/v), 1% SDS, and 31 μM β-mercaptoethanol) at 100C for 5 min., separated on 12 % polyacrylamide gels, and transferred onto PVDF membranes as described [23-25]. The membranes were blocked in 5 % non-fat dry milk and incubated with primary antibodies (Cell Signaling Systems, 1:2, 000) at room temperature for 4-5 h, washed in 0.1 % Tween-20 containing buffer, incubated in goat anti-rabbit HRP conjugate (1:4,000) as described [23-25]. The antigen-antibody complexes were visualized by an enhanced chemiluminescence, ECL III detection kit (GE Health Care). Densitometry was performed using the NIH's ImageJ software.

2.10. Serum estradiol assay

Serum estradiol was measured using a mouse ELISA kit (Calbiotech, ES180S-100) according to the manufacturer's instructions. The concentration of the lowest standard measured was 3 pg/ml.

2.11. Statistics

For each experiment, 4-5 female *Fshb* null mice per group or 5-6 males were used. Data were reported as Mean ± SEM. Statistical analysis was performed by Graph Pad Prism software and included Student's T-test or one-way ANOVA followed by Turkey's post-hoc test. A P value < 0.05 was considered significant.

3. Results

3.1. Hypo ($FSH^{21/18}$)- and fully (FSH^{24})-glycosylated FSH glycoforms elicit dose-and time-dependent changes in gene expression in ovaries of Fshb null female mice

FSH is essential for ovarian folliculogenesis and *Fshb* null female mice develop a preantral stage block in ovarian folliculogenesis [21-24]. Many FSH-responsive genes remain suppressed in the ovaries of *Fshb* null mice [24, 27, 28]. In addition to the expression of well-known FSH-responsive genes, *Cyp19a1*, *Inhba* and *Inhbb*, we evaluated *Apaf1*, *S100g*, *Dok1*, *Kcnj8* marker genes. These marker genes were chosen because, the corresponding mRNAs were markedly upregulated in ovaries of *Fshb* null mice that were either pharmacologically [27, 29] or genetically [24] rescued. To test the *in vivo* bioactivities of

FSH$^{21/18}$ and FSH^{24}, we first ip injected 1 μg of the recombinant hormones separately (~ equivalent to 10 IU based on highly purified human FSH Reference Standard, with an estimated potency of 8.6 -10 mIU/ng) and tested the ovarian gene responses after 2h, 4h, 8h, 16h and 24h by Taqmman real-time qPCR assays. Expression of 5 (*Cyp19a1*, *Inhba*, *Inhbb*, *Ccnd1* and *Ki67*) out of the 9 (56 %) genes tested was significantly up-regulated by 2h compared to that at all other time points analyzed (Fig. 2). The induction of this set of genes was similar irrespective of whether FSH$^{21/18}$ or FSH^{24} glycoform was injected into *Fshb* null female mice (Fig. 2). In the absence of FSH, *Fshr* expression is normally up-regulated and injection of either FSH glycoform suppressed the expression after 2h (Fig. 2). In order to determine whether 2h represented the optimal time-point, we next tested the response to injection of a fixed 1μg dose of the recombinant hormones by assaying ovarian gene expression after 0.5h, 1h and 2h (Fig. 3). We first compared the responses to FSH^{21} and FSH^{24} with respect to time (after 2h) in a single qPCR assay and measured the expression of a set of 9 known FSH-responsive genes (Fig. 3).

Based on the initial gene expression profiling described above, we measured the ovarian gene expression more comprehensively by testing expression of 11 additional genes thus, evaluating the response of 20 genes to a 1 μg dose of FSH$^{21/18}$ or FSH^{24} and plotted the data separately with respect to different time points 0.5h, 1h and 2h, after injection (Fig. 4). When the expression changes of 60 genes (3 time points and 20 genes per time point) were collectively compared, it was evident that the FSH$^{21/18}$ glycoform induced 14 genes significantly higher than the FSH^{24} glycoform (23 %). The FSH^{24} glycoform induced 16 genes significantly higher than FSH$^{21/18}$ (27 %) and 30 genes (50 %) were nearly equally induced by both FSH glycoforms (Fig. 4). At a fixed time point of 2h, changing the dose of the hormones towards either the higher (2 μg) or lower (0.5 μg) end did not result in significantly higher expression responses in the majority of the ovarian genes than achieved with 1 μg of the hormones (Supplementary Fig. S2). Furthermore, two independent batches of the GH_3-derived recombinant FSH glycoform preparations were tested for their *in vivo* bioactivity. We found that both elicited identical ovarian gene responses in *Fshb* null female mice indicating no batch-to batch variation in bioactivities of the FSH glycoform preparations (data not shown). Together, these data indicate that hypo - glycosylated FSH$^{21/18}$, like fully-glycosylated FSH^{24} is bioactive *in vivo* and each FSH glycoform elicits temporally distinct gene responses in ovaries of *Fshb* null mice.

3.2. Differences in intra-ovarian signaling pathways regulated by FSH$^{21/18}$ and FSH^{24} glycoforms

FSH binds to and signals via GPCR-coupled FSH-receptors (FSHR) expressed on ovarian granulosa cells [30-32]. FSHR-mediated signaling leads to regulation of multiple downstream signaling pathways in granulosa cells including the CREB-dependent protein kinase-A (PKA) pathway [30, 33-35]. To determine if FSH$^{21/18}$ and FSH^{24} glycoforms elicit these responses in *Fshb* null females, first we tested ovarian expression of the activated forms of phospho-CREB and phospho-PKA substrate by qualitative immunofluorescence using specific antibodies. At a 1μg dose, both FSH$^{21/18}$ and FSH^{24} glycoforms induced expression of phospho-CREB and phospho-PKA substrate in ovarian granulosa cells compared to those in PBS-injected controls (Fig. 5). This induction occurred robustly at 30

minutes (Fig. 5 A, B) remained elevated at 1h (Fig. 5 C, D), and by 2h, minimal expression was observed in granulosa cells (Fig. 5 E, F).

We next tested expression of several FSH-R downstream signaling pathway components in ovarian lysates by Western blot analysis followed by densitometry. At a1μg dose, both $FSH^{21/18}$ and FSH^{24} glycoforms induced phospho-CREB and phospho-PKA substrate 30 min., 1h and 2h after injection, compared to that in PBS-injected controls (Fig. 6). Both glycoforms also significantly induced the expression of phospho-Akt at the three time points tested when compared to PBS-injected controls (Fig. 6). The maximal induction of phospho-Akt was achieved after 2h by treatment with hypo-glycosylated $FSH^{21/18}$ (Fig. 6 E, F). In contrast, striking differences were observed when induction of phosoho-p38 and phospho-p44/42 was compared. First, the hypo-glycosylated $FSH^{21/18}$ glycoform significantly induced phosoho-p38 after 30′ compared to fully-glycosylated FSH^{24} glycoform (Fig. 6 B). Hypo-glycosylated $FSH^{21/18}$ glycoform significantly induced phospho-p44/p42 only after 1h (Fig. 6D). Thus, the hypoglycosylated $FSH^{21/18}$ glycoform after 2h of treatment, significantly up-regulated expression of 4 of the 5 activated forms of FSH-R downstream signaling components in ovaries of *Fshb* null mice (Fig. 6F).

To test whether induction of FSH-R downstream signaling components by FSH glycoforms occurred before 30 minutes, we tested their expression at 5, 10 and 20 minutes after FSH glycoform injection. We found no significant induction of responses in the ovaries of *Fshb* null mice during these early time points after injection of the FSH glycoforms (Supplementary Fig. S3), although a trend towards upregulation was observed. Despite a better signaling response by the $FSH^{21/18}$ glycoform, both glycoforms induced a similar ovarian weight gain response (Fig. 7A). Moreover, ovarian histology by PAS/hematoxylin staining indicated that 1 μg of either $FSH^{21/18}$ or FSH^{24} glycoform induced antrum formation by 48h (Fig. 7 B-E). Interestingly, serum estradiol was significantly higher in $FSH^{21/18}$ glycoform - injected immature *Fshb* null females compared to that in either FSH^{24}-injected immature *Fshb* null females or PBS-injected immature control mice (Fig. 7F). Collectively, all the above data indicate that hypo-glycosylated $FSH^{21/18}$ is biologically active in inducing FSH-R downstream signaling pathway components and estradiol production from ovaries of *Fshb* null mice, similar to that by fully-glycosylated FSH^{24}.

3.3. In vivo bioactivities of $FSH^{21/18}$ and FSH^{24} glycoforms in Fshb null male mice

FSH binds to G-protein coupled FSH-receptors on Sertoli cells in the testis. FSH regulates Sertoli cell proliferation during pre-pubertal testis development [36-38]. Adult *Fshb* null male mice display reduced testis weight as a result of fewer Sertoli cells [39, 40]. To evaluate *in vivo* bioactivity of FSH glycoforms in the male, beginning at postnatal day 5, mice were injected once daily with either PBS, $FSH^{21/18}$ or FSH^{24} for 5 days. By postnatal day 10, testis weights in PBS-injected *Fshb* null mice significantly increased compared with those at 5d (Fig. 8A). Compared to the PBS injected group, FSH glycoform-injected groups demonstrated a significant increase in testicular weights on postnatal day10. When injected with $FSH^{21/18}$, testis weights in *Fshb* null mice increased by 1.8 times (3.8 times compared to that in PBS injected *Fshb* null mice on postnatal day 5) by d10 (Fig. 8A). When injected with FSH^{24}, testis weights in *Fshb* null mice increased by 1.3 times (2.6 times compared to

PBS injected controls on postnatal day 5) (Fig. 8A). When testis weight gain responses were compared between the two FSH glycoforms, although the hypo-glycosylated $FSH^{21/18}$ glycoform showed a greater response (1.4-1.5 times more) than that by the full-glycosylated FSH^{24} glycoform, it was not statistically significant (Fig. 8A).

Consistent with the above testis weight data, histological analysis of hematoxylin - eosin-stained testis sections indicated that testis tubule size significantly increased in FSH glycoform-treated mice compared to those in PBS-injected *Fshb* null males (Fig. 8B). Further, immunolabeling with an antibody against GCNA1, a pan-germ cell marker showed that a greater number of germ cells were present in the testis sections from FSH glycoform - injected *Fshb* null mice compared to those in PBS - injected group (Fig. 8C) likely as a result of more number of Sertoli cells. Both the testis tubule size (Fig. 8B, right most panel, bar graph) and germ cell number (Fig. 8C, right most panel, bar graph) were significantly higher in testes of mice treated with $FH^{21/18}$ compared to that by FSH^{24}. Finally, expression analysis of FSH-responsive genes in testis by qPCR assays (Fig. 8D) indicated that the $FSH^{21/18}$ glycoform significantly upregulated 4 (*Cdo1*, *Clu*, *Tbx22* and *Zic3*) out of the 9 (44 %) and down-regulated 1 (*Amh*) out of the 9 (11 %) and did not affect 4 (*Car13*, *Fshr*, *Gsta2*, *Slc12a5*) out of the 9 (44 %) genes. In contrast, only 1 out of the 9 (11%) genes was significantly up- (*Car13*) and downregulated (*Fshr*) by FSH^{24}. 3 (*Cdo1*, *Tbx22*, and *Amh*) out of the 9 genes (33 %) were not affected by only FSH^{24}. Two (*Gsta2* and *Slc12a5*) out of the 9 (22 %) genes were unaffected by either of the FSH glycoform and their expression was nearly identical to that in testes of the PBS-injected control group (Fig. 8D).

Because, Sertoli cells in the mouse testis begin to cease to proliferate by postnatal day 10, we assayed Sertoli cell proliferation by *in vivo* BrdU labeling in testes of postnatal day 5 pups that received daily injections of FSH glycoforms for 3 days beginning postnatal day 3 (Supplementary Fig. 1 C and Fig. 8E). In the absence of FSH, Sertoli cell proliferation was significantly reduced by 45 % in *Fshb* null mice (Fig. 8F). Scoring the percentage of proliferating $Sox9^{+}/BrdU^{+}$ Sertoli cells confirmed that FSH glycoforms significantly enhanced the Sertoli cell proliferation in *Fshb* null mice. The hypo-glycosylated $FSH^{21/18}$ glycoform significantly enhanced Sertoli cell proliferation when compared to that by fully-glycosylated FSH^{24} (Fig. 8F). Collectively, all the above data confirm that both FSH glycoforms are bioactive *in vivo* in *Fshb* null males in the absence of endogenous FSH. Furthermore, the hypo-glycosylated $FSH^{21/18}$ glycoform elicited a better response than the fully-glycosylated FSH^{24} glycoform when testis tubule size and Sertoli cell proliferation were quantified.

4. Discussion

The existence of macro-heterogeneity in FSH preparations contributed by FSHβ subunits differing in N-glycosylation was recently confirmed [4-6, 14, 17-19]. Four FSH glycoforms were identified by direct purification from pituitary extracts [4-7, 14, 17-19] and following recombinant expression of genes encoding specific N-glycosylation mutant FSHβ subunits [4-7, 14, 17-19]. Both hypo-glycosylated $FSH^{21/18}$ and fully-glycosylated FSH^{24} glycoform preparations were tested *in vitro* in radio-ligand and radio-receptor assays [4, 6, 18] and immortalized granulosa cell cultures [17]. In many of these *in vitro* assays, the hypo-

glycosylated $FSH^{21/18}$ glycoform preparation was found more active than the fully-glycosylated FSH^{24} glycoform preparation [4, 6, 17, 18]. It has also been proposed that the abundance of FSH glycoforms in tissue, serum and urine changes with age and could have implications for ovarian aging and for explaining at least some of the extra-gonadal actions of FSH [4, 14, 17-19]. However, whether these different FSH glycoforms elicit bioactivity *in vivo* and if there are differences in their *in vivo* bioactivity had not been tested to date.

Here, we have tested the recombinant GH_3 cell-derived FSH glycoform preparations ($FSH^{21/18}$ and FSH^{24}) by a pharmacological rescue strategy using immature *Fshb* null female mice. This strategy permitted us to monitor the *in vivo* bioactivity of the injected FSH glycoforms on an identical *Fshb* null genetic background and in the absence of endogenous FSH. We took advantage of our previously made observation that *Fshb* null mice retain full FSH-responsiveness to exogenous FSH [22] and these mice could be rescued both genetically [21, 23, 24] and pharmacologically [22, 41, 42]. Our data in this manuscript are consistent with these previously published reports and confirm that the GH_3-cell-derived recombinant FSH glycosylation variants are biologically active *in vivo*. As our candidate gene expression data set represents only a “snapshot” of the known FSH-responsive genes in the mouse ovary [27, 28], additional studies employing large-scale gene expression profiling such as microarray/RNA Seq techniques are required to completely characterize large-scale responses elicited by each FSH glycoform.

$FSH^{21/18}$ and FSH^{24} glycoforms differently regulated 20 genes in the ovary whose expression was analyzed after 2h of treatment by real-time PCR. We could place these genes into distinct biological pathways, thereby implicating that $FSH^{21/18}$ and FSH^{24} glycoforms act via different pathways *in vivo*. Based on these gene responses to different FSH glycoforms, we predict that the $FSH^{21/18}$ glycoforms may regulate cell cycle, apoptosis, cell adhesion events and growth factor-mediated signaling. The FSH^{24} glycoform may regulate cell differentiation pathways and transcription factor-mediated events. In support of this, the $FSH^{21/18}$ and FSH^{24} glycoforms also induced expression of different activated forms of key signaling pathways downstream of FSH-receptors. Whether the observed differences manifest and are indicative of *in vivo* clearance rates of each hormone is not known. Recombinant hFSH glycosylation mutants equivalent to FSH^{21} and FSH^{18} were reported to be cleared from rat serum significantly faster than wild-type FSH, which was probably an 80%/20% mixture of FSH^{24} and $FSH^{21/18}$ [43]. More detailed kinetic studies involving tracer-labeled glycoform preparations injected into *Fshb* null mice and monitoring of their clearance in mouse blood need to be performed to correlate these gene expression differences to glycoform serum half-lives. Nevertheless, our *in vivo* bioactivity data including estradiol production are in close agreement with recent *in vitro* data that also demonstrate that hypo-glycosylated FSH is more active than fully-glycosylated FSH in a granulosa tumor-derived KGN cell line [17]. Together, the previous *in vitro* [6, 17, 18] and *in vivo* bioactivity data in this manuscript functionally validate the biochemical data that indicated enhanced receptor occupancy and high affinity binding by hypo-glycosylated FSH glycoforms compared to those by the fully-glycosylated form [6, 17, 18]. These results stand in sharp contrast to studies with classic FSH isoforms which have differences in charge due to terminal sialic acids contributing to micro-heterogeneity in human FSH. Less acidic FSH isoforms exhibited significantly higher *in vivo* biological activity than more acidic FSH

isoforms [44, 45]. Studies in the sheep model have indicated that acidic mix of FSH isoforms were more potent in inducing follicular maturation and estradiol production than the less acidic isoforms [46, 47]. Thus, it appears that the ratio of different FSH glycoforms may be important for *in vivo* biological actions of FSH [16].

We previously showed that daily injections of recombinant FSH to neonatal *Fshb* null male pups resulted in an increase in testis weights compared to those in *Fshb* null pups injected with PBS [48]. We modified this protocol and injected different FSH glycoforms once daily for 5 days, beginning at postnatal day 5. In this modified FSH *in vivo* bioassay in the male, each FSH glycoform was found active. The Sertoli cell proliferation was significantly higher in mice injected with $FSH^{21/18}$ as compared to those in FSH^{24} - injected mice. Since the number of Sertoli cells also dictates the germ cell- carrying capacity, more $GCNA1^{+}$ germ cells were present in FSH glycoform-injected mice.

We also found differences in testis gene expression in *Fshb* null males when injected with $FSH^{21/18}$ or FSH^{24} (Fig. 8). We evaluated expression of a set of candidate genes shown in Fig. 8D, because these were found to be FSH-responsive in mouse Sertoli cells during the proliferative phase (Wang H., and Kumar T.R., unpublished results) prior to puberty. Currently, we do not know the functional significance of these FSH-responsive genes in the mouse testis. Similar to what we observed in the ovary, it is likely that each glycoform may signal through different signaling pathways in the testis, resulting in changes in different networks of gene expression. For example, while the classical signaling pathway downstream of FSH receptor is the cAMP-CREB and PKA pathway, we previously reported that FSH acts via a non-classical MAPK pathway involving NF-κB transcription factor and regulates AMH production [48]. It would be interesting to determine in the future the different gene networks regulated by different FSH glycoforms in the testis. The ability to quantify the expression of different testicular genes in *Fshb* null males in response to different FSH glycoforms provides another convenient *in vivo* bioassay for testing different FSH analogs.

The existence of a naturally occurring hypo-glycosylated human FSH variant and its changing abundance with age have been reported [18]. The hypo-glycosylated variant was particularly abundant in younger women during ovulatory cycles [18] when rapid action and clearance were required [49]. Consistent with this, in a radioligand assay, hypo-glycosylated FSH exhibited faster kinetics and bound a higher number of FSH receptors on rat testicular homogenate, calf testis membranes and ovarian cells expressing hFSHRs, more rapidly than the fully-glycosylated FSH [6]. Recent *in vitro* studies also support these receptor binding studies. These studies showed that relatively low doses of hypo-glycosylated FSH more robustly induced cAMP, estradiol and progesterone production in cultured granulosa cells when compared to that by fully-glycosylated FSH glycoform [17]. Thus, it was proposed that loss of hypo-glycosylated FSH associated with aging may manifest in defective follicle maturation and oocyte development and ultimately result in loss of ovarian function [17, 18]. This loss of ovarian function leads to loss of estrogen production and results in production of elevated fully-glycosylated FSH glycoform, whose abundance predominates over the hypo-glycosylated FSH during peri- or post-menopausal age [17, 18]. It is possible that the hypo- and fully-glycosylated FSH glycoforms may signal differently and exhibit a biased agonism

at the FSHR in granulosa cells. Such a likely biased agonism by gonadotropin glycoforms at the level of cellular responses has been previously reported [50-53].

Non-classical FSH action other than cAMP-PKA pathway has been reported in Sertoli cells [48], bone osteoclasts [54] and more recently in myometrial [55] and endometrial cells [56]. Because FSH-receptors have been identified on non-gonadal cells including bone osteoclasts [54], tumor blood vessels [57], and uterine and placental cells [55, 56, 58, 59], it would be interesting to determine whether different FSH glycoforms bind and signal via FSH receptors in these non-gonadal cells. Most likely, $FSH^{21/18}$ and FSH^{24} glycoforms may signal through different pathways in these different cell types. Because the ratio of $FSH^{21/18}$ to FSH^{24} and the tissue/cell specificity of FSH action changes with age, biased agonism could be one mechanism through which these different FSH ligands signal via FSHRs and utilize different downstream components. These possibilities need to be tested in the future using both *in vitro* and *in vivo* approaches.

In conclusion, we tested the *in vivo* bioactivities of the hypo-glycosylated $FSH^{21/18}$ and fully-glycosylated FSH^{24} glycoforms using a pharmacological rescue approach involving *Fshb* null mice. Our studies confirm that the FSH glycoforms elicit FSH bioactivity *in vivo* as measured by ovarian and testicular gene expression responses. Our *in vivo* studies in the male reveal that $FSH^{21/18}$ is more efficacious than FSH^{24}. Our studies in the female demonstrate that each glycoform participates in a different downstream signaling pathway in the ovary. Changes in abundance of different FSH glycoforms could explain their age-specific actions in target tissues for example, ovary versus bone [14, 17]. The long-term *in vivo* effects of distinct FSH glycoforms and their age-specific abundance will be of considerable interest in the future for testing their efficacy in follicle maturation protocols and further evaluating the associated clinical benefits.

Supplementary Material

Refer to Web version on PubMed Central for supplementary material.

Acknowledgments

We thank Dr. Irving Boime for his generous gift of the hFSH-expressing GH_3 cell line. We thank Dr. Jean-Michel Bidart for monoclonal antibodies RFSH20 and HT13, Dr. James A. Dias for monoclonal antibody 46.3 H6. B7 used in the recombinant FSH purification studies. This research work was funded in part by an NIH grant P01AG 029531 (to T.R.K. and G.R.B.), a KINBRE Bridge Grant P20GM103418 (to T.R.K.) and Edgar L. and Patricia Makowski Endowment funds (to T.R.K.).

Abbreviations

AMH	anti-Müllerian hormone
cAMP	Cyclic adenosine 5′-monophosphate
CHO	Chinese hamster ovary
CREB	Cyclic AMP-responsive element binding protein
FSH	Follicle-stimulating hormone

LH	Luteinizing hormone
PKA	Protein kinase-A
PVDF	Polyvinylidine difluoride
RIA	Radioimmuno assay
RRA	Radioreceptor assay
r-h	Recombinant human

References

1. Bousfield, GR.; Jia, L.; Ward, DN. Gonadotropins: chemistry and biosynthesis. In: Neill, JD., editor. Knobil and Neill's Physiology of Reproduction. 3rd ed. Vol. 1. Elsevier Press; New York: 2006. p. 1581-1634.
2. Pierce JG, Parsons TF. Glycoprotein hormones: structure and function. Annu Rev Biochem. 1981; 50:465–495. [PubMed: 6267989]
3. Baenziger JU, Green ED. Pituitary glycoprotein hormone oligosaccharides: structure, synthesis and function of the asparagine-linked oligosaccharides on lutropin, follitropin and thyrotropin. Biochim Biophys Acta. 1988; 947:287–306. [PubMed: 3130893]
4. Bousfield GR, Butnev VY, Rueda-Santos MA, Brown A, Hall AS, Harvey DJ. Macro and Micro-heterogeneity in Pituitary and Urinary Follicle-Stimulating Hormone Glycosylation. J Glycomics Lipidomics. 2014; 4
5. Bousfield GR, Butnev VY, White WK, Hall AS, Harvey DJ. Comparison of Follicle-Stimulating Hormone Glycosylation Microheterogenity by Quantitative Negative Mode Nano-Electrospray Mass Spectrometry of Peptide-N Glycanase-Released Oligosaccharides. J Glycomics Lipidomics. 2015; 5
6. Butnev VY, Butnev VY, May JV, Shuai B, Tran P, White WK, Brown A, Smalter Hall A, Harvey DJ, Bousfield GR. Production, purification, and characterization of recombinant hFSH glycoforms for functional studies. Mol Cell Endocrinol. 2015; 405:42–51. [PubMed: 25661536]
7. Dalpathado DS, Irungu J, Go EP, Butnev VY, Norton K, Bousfield GR, Desaire H. Comparative glycomics of the glycoprotein follicle stimulating hormone: glycopeptide analysis of isolates from two mammalian species. Biochemistry. 2006; 45:8665–8673. [PubMed: 16834341]
8. Gervais A, Hammel YA, Pelloux S, Lepage P, Baer G, Carte N, Sorokine O, Strub JM, Koerner R, Leize E, Van Dorsselaer A. Glycosylation of human recombinant gonadotrophins: characterization and batch-to-batch consistency. Glycobiology. 2003; 13:179–189. [PubMed: 12626416]
9. Grass J, Pabst M, Chang M, Wozny M, Altmann F. Analysis of recombinant human follicle-stimulating hormone (FSH) by mass spectrometric approaches. Anal Bioanal Chem. 2011; 400:2427–2438. [PubMed: 21461863]
10. Lombardi A, Andreozzi C, Pavone V, Triglione V, Angiolini L, Caccia P. Evaluation of the oligosaccharide composition of commercial follicle stimulating hormone preparations. Electrophoresis. 2013; 34:2394–2406. [PubMed: 23775770]
11. Wang H, Chen X, Zhang X, Zhang W, Li Y, Yin H, Shao H, Chen G. Comparative Assessment of Glycosylation of a Recombinant Human FSH and a Highly Purified FSH Extracted from Human Urine. J Proteome Res. 2016; 15:923–932. [PubMed: 26812091]
12. Anobile CJ, Talbot JA, McCann SJ, Padmanabhan V, Robertson WR. Glycoform composition of serum gonadotrophins through the normal menstrual cycle and in the post-menopausal state. Mol Hum Reprod. 1998; 4:631–639. [PubMed: 9701785]
13. Creus S, Pellizzari E, Cigorraga SB, Campo S. FSH isoforms: bio and immuno-activities in post-menopausal and normal menstruating women. Clin Endocrinol (Oxf). 1996; 44:181–189. [PubMed: 8849573]

14. Davis JS, Kumar TR, May JV, Bousfield GR. Naturally Occurring Follicle-Stimulating Hormone Glycosylation Variants. J Glycomics Lipidomics. 2014; 4:e117. [PubMed: 25893134]
15. Loreti N, Ambao V, Juliato CT, Machado C, Bahamondes L, Campo S. Carbohydrate complexity and proportion of serum FSH isoforms reflect pituitary-ovarian activity in perimenopausal women and depot medroxyprogesterone acetate users. Clin Endocrinol (Oxf). 2009; 71:558–565. [PubMed: 19250269]
16. Padmanabhan V, Lee JS, Beitins IZ. Follicle-stimulating isohormones: regulation and biological significance. J Reprod Fertil Suppl. 1999; 54:87–99. [PubMed: 10692847]
17. Jiang C, Hou X, Wang C, May JV, Butnev VY, Bousfield GR, Davis JS. Hypoglycosylated hFSH Has Greater Bioactivity Than Fully Glycosylated Recombinant hFSH in Human Granulosa Cells. J Clin Endocrinol Metab. 2015; 100:E852–860. [PubMed: 25915568]
18. Bousfield GR, Butnev VY, Butnev VY, Hiromasa Y, Harvey DJ, May JV. Hypo glycosylated human follicle-stimulating hormone (hFSH(21/18)) is much more active in vitro than fully-glycosylated hFSH (hFSH(24)). Mol Cell Endocrinol. 2014; 382:989–997. [PubMed: 24291635]
19. Bousfield GR, Butnev VY, Walton WJ, Nguyen VT, Huneidi J, Singh V, Kolli VS, Harvey DJ, Rance NE. All-or-none N-glycosylation in primate follicle-stimulating hormone beta-subunits. Mol Cell Endocrinol. 2007; 260:262–40.
20. Green ED, Boime I, Baenziger JU. Differential processing of Asn-linked oligosaccharides on pituitary glycoprotein hormones: implications for biologic function. Mol Cell Biochem. 1986; 72:81–100. [PubMed: 3102943]
21. Kumar TR, Low MJ, Matzuk MM. Genetic rescue of follicle-stimulating hormone beta-deficient mice. Endocrinology. 1998; 139:3289–3295. [PubMed: 9645705]
22. Kumar TR, Wang Y, Lu N, Matzuk MM. Follicle stimulating hormone is required for ovarian follicle maturation but not male fertility. Nat Genet. 1997; 15:201–204. [PubMed: 9020850]
23. Wang H, Butnev V, Bousfield GR, Kumar TR. A human FSHB transgene encoding the double N-glycosylation mutant (Asn Asn) FSHbeta subunit fails to rescue Fshb null mice. Mol Cell Endocrinol. 2016
24. Wang H, Larson M, Jablonka-Shariff A, Pearl CA, Miller WL, Conn PM, Boime I, Kumar TR. Redirecting intracellular trafficking and the secretion pattern of FSH dramatically enhances ovarian function in mice. Proc Natl Acad Sci U S A. 2014; 111:5735–5740. [PubMed: 24706813]
25. Wang H, Graham I, Hastings R, Gunewardena S, Brinkmeier ML, Conn PM, Camper SA, Kumar TR. Gonadotrope-specific deletion of Dicer results in severely suppressed gonadotropins and fertility defects. J Biol Chem. 2015; 290:2699–2714. [PubMed: 25525274]
26. Wang H, Hastings R, Miller WL, Kumar TR. Fshb-iCre mice are efficient and specific Cre deleters for the gonadotrope lineage. Mol Cell Endocrinol. 2015
27. Burns KH, Yan C, Kumar TR, Matzuk MM. Analysis of ovarian gene expression in follicle-stimulating hormone beta knockout mice. Endocrinology. 2001; 142:2742–2751. [PubMed: 11415992]
28. Harlow CR, Davidson L, Burns KH, Yan C, Matzuk MM, Hillier SG. FSH and TGF-beta superfamily members regulate granulosa cell connective tissue growth factor gene expression in vitro and in vivo. Endocrinology. 2002; 143:3316–3325. [PubMed: 12193543]
29. Burns KH, Owens GE, Ogbonna SC, Nilson JH, Matzuk MM. Expression profiling analyses of gonadotropin responses and tumor development in the absence of inhibins. Endocrinology. 2003; 144:4492–4507. [PubMed: 12959983]
30. Hunzicker-Dunn M, Maizels ET. FSH signaling pathways in immature granulosa cells that regulate target gene expression: branching out from protein kinase A. Cell Signal. 2006; 18:1351–1359. [PubMed: 16616457]
31. Ryan RJ, Birnbaumer L, Lee CY, Hunzicker-Dunn M. Gonadotropin interactions with the gonad as assessed by receptor binding and adenylyl cyclase activity. Int Rev Physiol. 1977; 13:85–152. [PubMed: 191421]
32. Tao YX, Segaloff DL. Follicle stimulating hormone receptor mutations and reproductive disorders. Prog Mol Biol Transl Sci. 2009; 89:115–131. [PubMed: 20374735]
33. Richards JS. Hormonal control of gene expression in the ovary. Endocr Rev. 1994; 15:725–751. [PubMed: 7705279]

34. Richards JS, Pangas SA. New insights into ovarian function. Handb Exp Pharmacol. 2010:3–27. [PubMed: 20839083]
35. Richards JS, Russell DL, Ochsner S, Hsieh M, Doyle KH, Falender AE, Lo YK, Sharma SC. Novel signaling pathways that control ovarian follicular development, ovulation, and luteinization. Recent Prog Horm Res. 2002; 57:195–220. [PubMed: 12017544]
36. Franca LR, Hess RA, Dufour JM, Hofmann MC, Griswold MD. The Sertoli cell: one hundred fifty years of beauty and plasticity. Andrology. 2016; 4:189–212. [PubMed: 26846984]
37. Griswold MD. The central role of Sertoli cells in spermatogenesis. Semin Cell Dev Biol. 1998; 9:411–416. [PubMed: 9813187]
38. Griswold MD, Heckert L, Linder C. The molecular biology of the FSH receptor. J Steroid Biochem Mol Biol. 1995; 53:215–218. [PubMed: 7626457]
39. Kumar TR, Varani S, Wreford NG, Telfer NM, de Kretser DM, Matzuk MM. Male reproductive phenotypes in double mutant mice lacking both FSHbeta and activin receptor IIA. Endocrinology. 2001; 142:3512–3518. [PubMed: 11459797]
40. Wreford NG, Rajendra Kumar T, Matzuk MM, de Kretser DM. Analysis of the testicular phenotype of the follicle-stimulating hormone beta-subunit knockout and the activin type II receptor knockout mice by stereological analysis. Endocrinology. 2001; 142:2916–2920. [PubMed: 11416011]
41. Garcia-Campayo V, Boime I, Ma X, Daphna-Iken D, Kumar TR. A single-chain tetradomain glycoprotein hormone analog elicits multiple hormone activities in vivo. Biol Reprod. 2005; 72:301–308. [PubMed: 15385421]
42. Garcia-Campayo V, Kumar TR, Boime I. Thyrotropin, follitropin, and chorionic gonadotropin expressed as a single multifunctional unit reveal remarkable permissiveness in receptor-ligand interactions. Endocrinology. 2002; 143:3773–3778. [PubMed: 12239087]
43. Bishop LA, Nguyen TV, Schofield PR. Both of the beta-subunit carbohydrate residues of follicle-stimulating hormone determine the metabolic clearance rate and in vivo potency. Endocrinology. 1995; 136:2635–2640. [PubMed: 7750487]
44. Ulloa-Aguirre A, Timossi C, Barrios-de-Tomasi J, Maldonado A, Nayudu P. Impact of carbohydrate heterogeneity in function of follicle-stimulating hormone: studies derived from in vitro and in vivo models. Biol Reprod. 2003; 69:379–389. [PubMed: 12700183]
45. Wide L, Hobson B. Influence of the assay method used on the selection of the most active forms of FSH from the human pituitary. Acta Endocrinol (Copenh). 1986; 113:17–22. [PubMed: 3094307]
46. Padmanabhan V, Mieher CD, Borondy M, I'Anson H, Wood RI, Landefeld TD, Foster DL, Beitins IZ. Circulating bioactive follicle-stimulating hormone and less acidic follicle-stimulating hormone isoforms increase during experimental induction of puberty in the female lamb. Endocrinology. 1992; 131:213–220. [PubMed: 1611999]
47. West CR, Carlson NE, Lee JS, McNeilly AS, Sharma TP, Ye W, Padmanabhan V. Acidic mix of FSH isoforms are better facilitators of ovarian follicular maturation and E2 production than the less acidic. Endocrinology. 2002; 143:107–116. [PubMed: 11751599]
48. Lukas-Croisier C, Lasala C, Nicaud J, Bedecarras P, Kumar TR, Dutertre M, Matzuk MM, Picard JY, Josso N, Rey R. Follicle-stimulating hormone increases testicular Anti-Mullerian hormone (AMH) production through sertoli cell proliferation and a nonclassical cyclic adenosine 5'-monophosphate-mediated activation of the AMH Gene. Mol Endocrinol. 2003; 17:550–561. [PubMed: 12554789]
49. Wide L, Eriksson K. Dynamic changes in glycosylation and glycan composition of serum FSH and LH during natural ovarian stimulation. Ups J Med Sci. 2013; 118:153–164. [PubMed: 23527482]
50. Dahl KD, Bicsak TA, Hsueh AJ. Naturally occurring antihormones: secretion of FSH antagonists by women treated with a GnRH analog. Science. 1988; 239:72–74. [PubMed: 3122320]
51. Timossi CM, Barrios de Tomasi J, Zambrano E, Gonzalez R, Ulloa-Aguirre A. A naturally occurring basically charged human follicle-stimulating hormone (FSH) variant inhibits FSH-induced androgen aromatization and tissue-type plasminogen activator enzyme activity in vitro. Neuroendocrinology. 1998; 67:153–163. [PubMed: 9630432]

52. Timossi CM, Barrios-de-Tomasi J, Gonzalez-Suarez R, Arranz MC, Padmanabhan V, Conn PM, Ulloa-Aguirre A. Differential effects of the charge variants of human follicle-stimulating hormone. J Endocrinol. 2000; 165:193–205. [PubMed: 10810283]

53. Wehbi V, Tranchant T, Durand G, Musnier A, Decourtye J, Piketty V, Butnev VY, Bousfield GR, Crepieux P, Maurel MC, Reiter E. Partially deglycosylated equine LH preferentially activates beta-arrestin-dependent signaling at the follicle-stimulating hormone receptor. Mol Endocrinol. 2010; 24:561–573. [PubMed: 20107152]

54. Sun L, Peng Y, Sharrow AC, Iqbal J, Zhang Z, Papachristou DJ, Zaidi S, Zhu LL, Yaroslavskiy BB, Zhou H, Zallone A, Sairam MR, et al. FSH directly regulates bone mass. Cell. 2006; 125:247–260. [PubMed: 16630814]

55. Stilley JA, Guan R, Santillan DA, Mitchell BF, Lamping KG, Segaloff DL. Differential Regulation of Human and Mouse Myometrial Contractile Activity by FSH as a Function of FSH Receptor Density. Biol Reprod. 2016

56. Ponikwicka-Tyszko D, Chrusciel M, Stelmaszewska J, Bernaczyk P, Sztachelska M, Sidorkiewicz I, Doroszko M, Tomaszewski J, Tapanainen JS, Huhtaniemi I, Wolczynski S, Rahman NA. Functional Expression of FSH Receptor in Endometriotic Lesions. J Clin Endocrinol Metab. 2016; 101:2905–2914. [PubMed: 27224263]

57. Radu A, Pichon C, Camparo P, Antoine M, Allory Y, Couvelard A, Fromont G, Hai MT, Ghinea N. Expression of follicle-stimulating hormone receptor in tumor blood vessels. N Engl J Med. 2010; 363:1621–1630. [PubMed: 20961245]

58. Stilley JA, Christensen DE, Dahlem KB, Guan R, Santillan DA, England SK, Al-Hendy A, Kirby PA, Segaloff DL. FSH receptor (FSHR) expression in human extragonadal reproductive tissues and the developing placenta, and the impact of its deletion on pregnancy in mice. Biol Reprod. 2014; 91:74. [PubMed: 25100706]

59. Stilley JA, Guan R, Duffy DM, Segaloff DL. Signaling through FSH receptors on human umbilical vein endothelial cells promotes angiogenesis. J Clin Endocrinol Metab. 2014; 99:E813–820. [PubMed: 24527712]

Highlights

- *In vivo* bioactivity of recombinant hypo ($FSH^{21/18}$) - and fully (FSH^{24}) - glycosylated FSH was tested in *Fshb*$^{-/-}$ mice.
- Both the FSH glycoforms elicited an ovarian weight gain response and induced antrum formation in *Fshb*$^{-/-}$ female mice.
- In ovarian gene induction assays, FSH glycoforms were found active in the absence of endogenous FSH.
- Both the FSH glycoforms elicited a testis weight gain response in *Fshb*$^{-/-}$ male mice.
- In Sertoli cell proliferation and testis gene expression assays, $FSH^{21/18}$ glycoform was found more active than FSH^{24}.

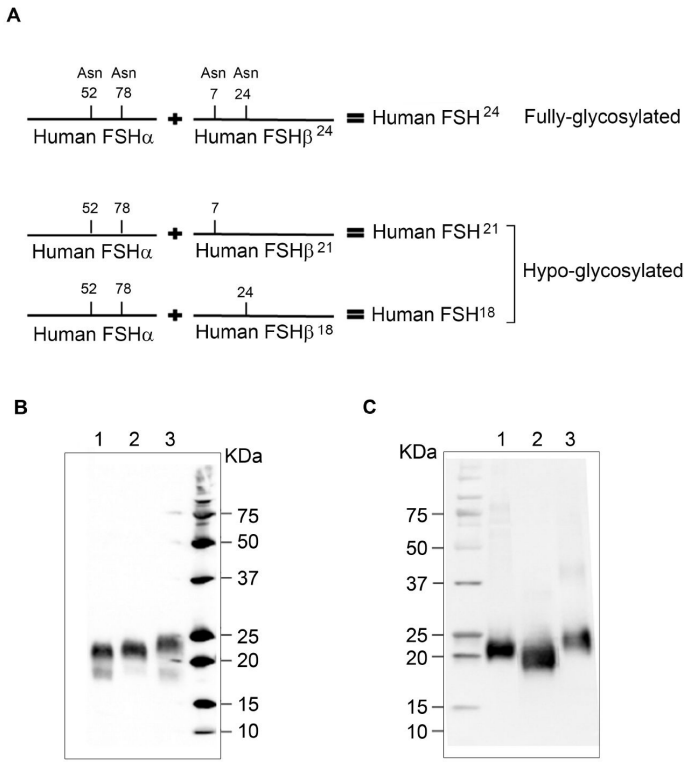

Fig. 1.

A summary of N-linked sugar chains attached at the Asn residues in human FSH subunits and the FSH glycoform nomenclature (A). Western blot analysis (B) using a mouse anti-human FSH monoclonal antibody (RFSH-20) indicates the molecular size of purified recombinant GH_3-derived $FSH^{21/18}$ and FSH^{24} glycoforms (Lanes 1 and 2). Purified human pituitary FSH reference preparation (AFP 7298) was used as positive control (Lane 3). An independent blot with FSH samples loaded in the same order as in panel B, was probed with an anti-alpha 15-2 monoclonal antibody (C).

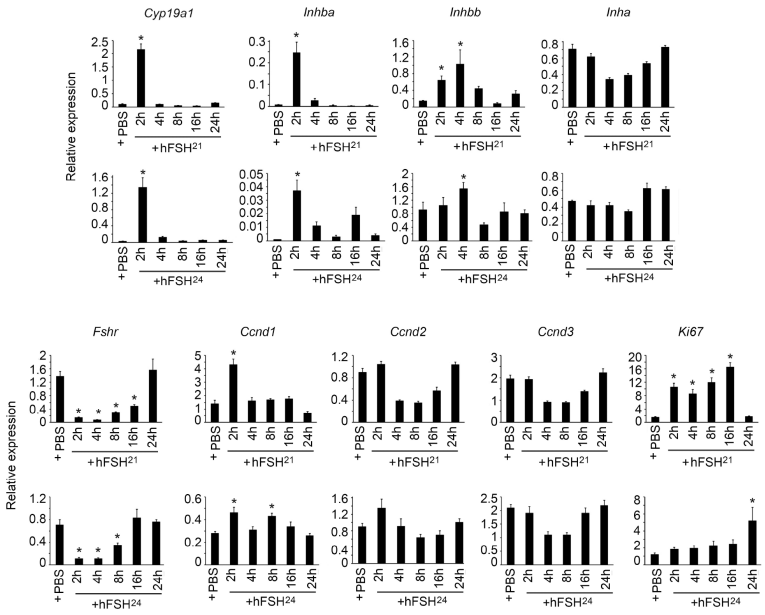

Fig. 2.

Ovarian gene expression analyzed by Taqman real time qPCR assays in *Fshb* null female mice injected with recombinant FSH glycoforms at 1μg dose. Gene expression was assayed between 2h – 24h at different time points. For each time point, triplicate cDNA samples from ovaries from 4-5 mice were used. * $P < 0.05$ *vs.* PBS-injected control group. The genes analyzed are listed in the Supplementary Material Table - 1.

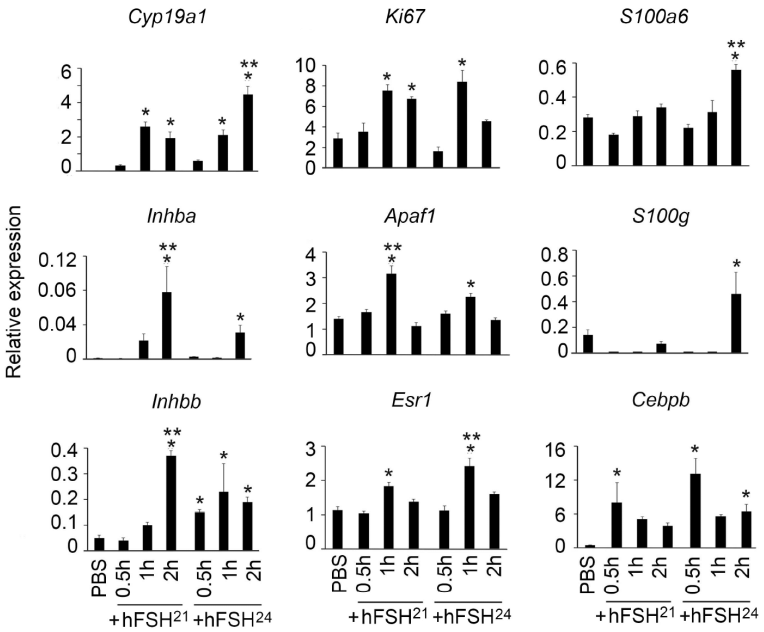

Fig. 3.

Ovarian gene expression analyzed by Taqman real time qPCR assays in *Fshb* null female mice injected with recombinant FSH glycoforms at 1μg dose. Gene expression was assayed at different time points between 0.5h – 2h as indicated. For each time point, triplicate cDNA samples from ovaries from 4-5 mice were used. * $P < 0.05$ *vs.* PBS-injected control group and ** $P < 0.05$ *vs.* the other glycoform at the same time point. The genes analyzed are listed in the Supplementary Material Table - 1.

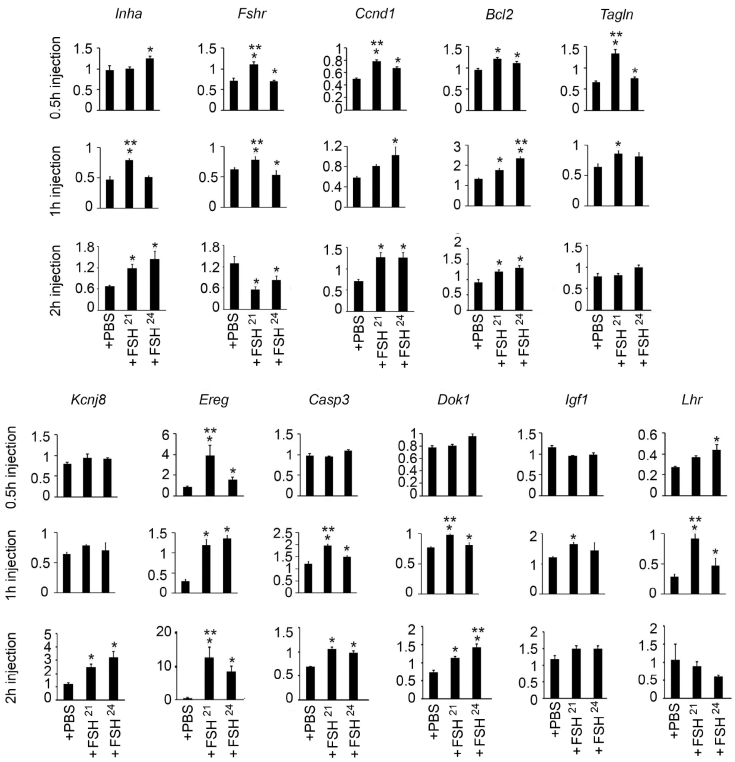

Fig. 4.

Ovarian gene expression analyzed by Taqman real time qPCR assays in *Fshb* null female mice injected with recombinant FSH glycoforms at 1μg dose. Expression of 11 known FSH-responsive marker genes was analyzed 0.5h, 1h and 2h after the FSH glycoform injection. Ovarian gene expression was separately compared for each time point. For each marker expression assay, triplicate cDNA samples from ovaries from 4-5 mice were used. * $P < 0.05$ *vs.* PBS-injected control group and ** $P < 0.05$ *vs.* the other glycoform. The genes analyzed are listed in the Supplementary Material Table - 1.

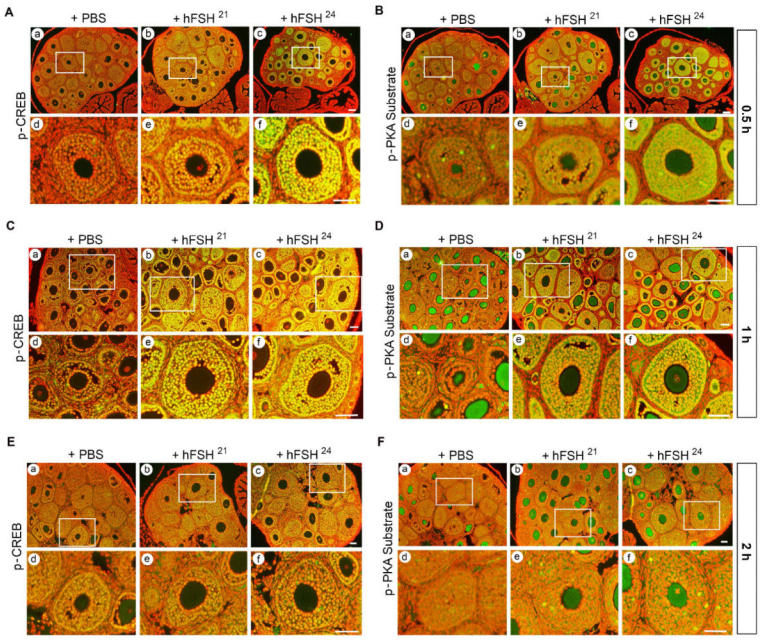

Fig. 5.

Immunolabeling of ovarian sections with anti-phospho-CREB (A, C and E) and anti-phospho-PKA substrate (B, D and F) antibodies indicate activation of FSH-receptor mediated signaling in ovaries of FSH glycoform injected *Fshb* null mice. Each FSH glycoform was injected at 1 μg dose and ovaries were harvested after 0.5h (A and B), 1h (C and D) and 2h (E and F), formalin-fixed and processed. Merged images are shown: specific antibody staining was visualized in green and the nuclei were stained red. Multiple sections from ovaries of 3 mice per group and per each time point were analyzed. Bottom panels represent enlarged images of follicles present in white squares in upper panels. White bar represents 100 μm.

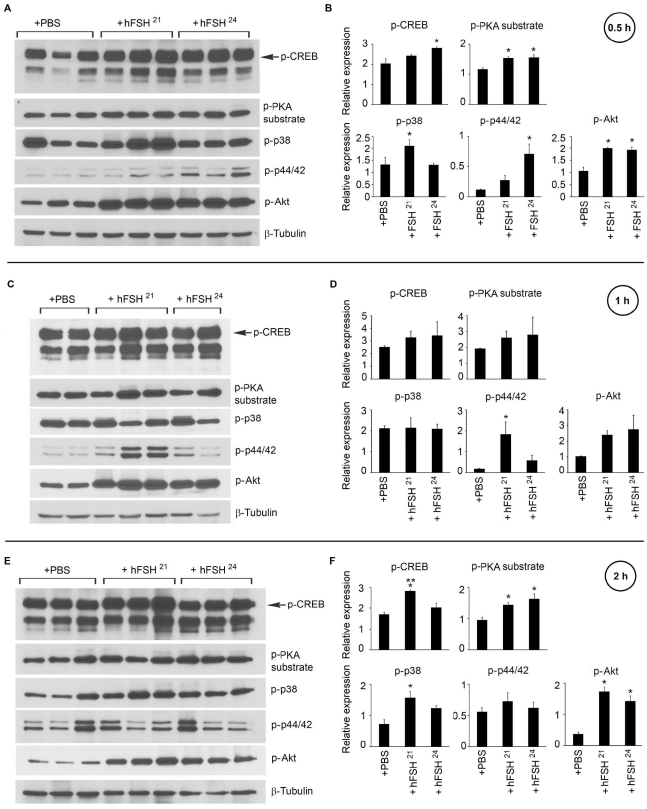

Fig. 6.

Western blot analysis of ovarian extracts probed with various antibodies against activated forms of signaling components downstream of FSH-receptor (A, C and E). Extracts were prepared from *Fshb* null mice injected with FSH glycoforms after different times (0.5h, 1h and 2h). Western blot analysis was performed on ovarian extracts from 2-3 mice per group and per time point. Expression of β-tubulin was used as an internal control and relative expression of each phospho-protein was plotted on the Y-axis. Densitometry data (B, D and F) represents an average of 3 independent blots. * $P < 0.05$ vs. PBS injected group and ** $P < 0.05$ *vs.* the other glycoform.

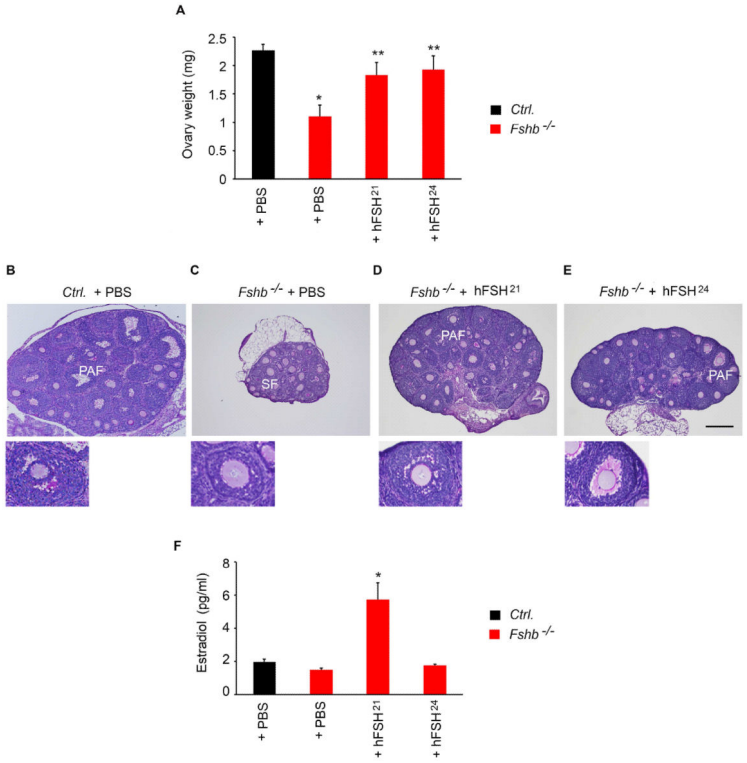

Fig. 7.

Loss of FSH results in hypoplastic ovaries and both the $FSH^{21/18}$ and FSH^{24} glycoforms elicit the ovarian weight gain response in *Fshb* null mice (A). Ovarian histology shows antrum in sections obtained from control (*Ctrl.*) (B) and FSH glycoform-injected (D and E) but not PBS-injected (C) $Fshb^{-/-}$ females. Serum estradiol was significantly high in $FSH^{21/18}$ injected immature *Fshb* null mice compared to either FSH^{24} - injected *Fshb* null females or PBS- injected control mice (F). * $P < 0.05$ *vs.* PBS-injected *Ctrl*, ** $P < 0.05$ *vs.* PBS-injected $Fshb^{-/-}$, n=6 mice per group. Black bar represents 200 μm.

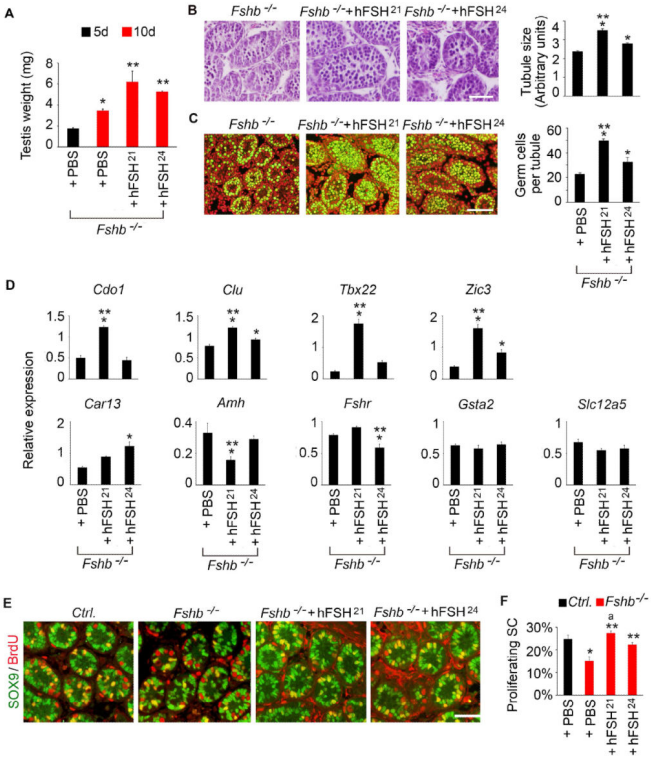

Fig. 8.

In vivo bioactivity of FSH glycoforms was evaluated following the protocols depicted in Supplementary Fig. S1. Both $FSH^{21/18}$ and FSH^{24} elicited a testis weight gain response in $Fshb^{-/-}$ male mice in a 5-day injection protocol (A). * $P < 0.05$ *vs.* 5d PBS group, ** $P <$ 0.05 vs. 10d PBS group, n=7 mice. Hematoxylin-eosin stained testis histology (B) shows increased number of germ cells in sections from $FSH^{21/18}$ - injected mice compared to those in FSH^{24} - injected mice resulting in increased tubule size (bar graph in panel B). Quantification of GCNA1, a pan-germ cell marker - positive germ cells by immunofluorescence indicates the same (C). In panel B and C, * P < 0.05 *vs.* PBS group, ** P < 0.05 *vs.* FSH^{24} group, n=3 mice, approximately 100 tubules were counted. White bar represents 100 μm in panel B and 200 μm in panel C. Taqman real time qPCR analysis (D) shows that 4 (*Cdo1*, *Clu Tbx22* and *Zic3*) out of the 9 FSH-responsive genes were upregulated by $FSH^{21/18}$ compared to FSH^{24}. * $P < 0.05$ vs. PBS group, ** $P < 0.05$ *vs.* the other glycoform. The genes analyzed are listed in the Supplementary Material Table -1. In panel E, testes sections from postnatal day 5 pups from control (*Ctrl.*) and experimental groups were immunolabeled with antibodies against SOX9, the Sertoli cell lineage - specific marker (green) and BrdU (red). The merged images are shown (E). White bar represents 200 μm. Quantification (F) shows that loss of FSH results in 45 % reduction in number of proliferating Sertoli cells (calculated as % of $Sox9^{+}BrdU^{+}$ /$Sox9^{+}$ cells) in $Fshb^{-/-}$ males. $FSH^{21/18}$ significantly increases the percentage of proliferating Sertoli cells in $Fshb^{-/-}$ males compared to those in FSH^{24} - injected $Fshb^{-/-}$ males (B). Approximately 250 tubules from multiple testis sections from 3 mice per group were counted. In panel F, * $P < 0.05$, *vs.* 5d *Ctrl.* group, ** $P < 0.05$ *vs.* 10d $Fshb^{-/-}$ group and [a] P < 0.05 *vs.* FSH^{24}-injected group.